Quasiparticle Dynamics in a Bose Insulator Probed by Interband Bragg Spectroscopy

N. Fabbri,[1,*] S. D. Huber,[2,†] D. Clément,[1,‡] L. Fallani,[1] C. Fort,[1] M. Inguscio,[1] and E. Altman[2]

[1]*LENS, Dipartimento di Fisica e Astronomia, Università di Firenze and INO-CNR, via Nello Carrara 1, I-50019 Sesto Fiorentino (FI), Italy*

[2]*Department of Condensed Matter Physics, The Weizmann Institute of Science, Rehovot, 76100, Israel*

(Received 6 September 2011; revised manuscript received 30 April 2012; published 31 July 2012)

We investigate experimentally and theoretically the dynamical properties of a Mott insulator in decoupled one-dimensional chains. Using a theoretical analysis of the Bragg excitation scheme, we show that the spectrum of interband transitions holds information on the single-particle Green's function of the insulator. In particular, the existence of particle-hole coherence due to quantum fluctuations in the Mott state is clearly seen in the Bragg spectra and quantified. Finally, we propose a scheme to directly measure the full, momentum-resolved spectral function as obtained in the angle-resolved photoemission spectroscopy of solids.

DOI: 10.1103/PhysRevLett.109.055301 PACS numbers: 67.85.Hj, 37.10.Jk, 67.85.De

The observation of the superfluid (SF) to Mott insulator (MI) transition of bosons in optical lattices [1] has received considerable attention as a paradigmatic example of a quantum phase transition driven by interactions. The properties of lattice bosons in this strongly correlated regime have been probed using several methods [2–10]. For example, time-of-flight experiments were used to study the development of spatial first-order coherence over increasing length scales inside the Mott state upon approaching the transition to the SF state [3]. In a quantum system, the emergence of such spatial correlations must go hand in hand with increasing temporal correlations. Near the quantum critical point, the precise relation between the two is determined by the dynamical critical exponent of the transition (see, e.g., Ref. [11]). Away from the transition, where critical properties are not yet apparent, the temporal first-order coherence lends insight on the nature of the quasiparticle excitations of the strongly correlated state.

So far, however, most of the dynamical experiments in the Mott regime using schemes of lattice modulation and Bragg spectroscopy have focused on excitation frequencies matching transition within the lowest-energy Bloch band [2,7]. In this case, the external perturbation is coupled to density fluctuations, and in the linear response regime, the absorption spectrum is directly related to the dynamical structure factor $S(q, \omega)$ of collective excitations, or particle-hole spectra [12–14].

In this Letter, we show how interband Bragg spectroscopy [7,15] supplemented by a theoretical model of the Mott insulator, can be used to extract properties of single-particle excitations in the many-body state. We then suggest a refined approach for directly measuring the single-particle Green's function in a model-independent way.

The MI state is realized in decoupled one-dimensional (1D) chains of interacting bosons, as represented in Fig. 1. We excite the system with two simultaneous laser pulses (Bragg beams) that induce an energy transfer $\hbar\omega = \hbar(\omega_1 - \omega_2)$ ($\omega_{1,2}$ being the laser beams frequencies) and a momentum transfer $\hbar\mathbf{q} = \hbar\mathbf{q}_1 - \hbar\mathbf{q}_2 = \hbar q \mathbf{e}_x$ along the axis of the 1D chains ($\mathbf{q}_1$ and $\mathbf{q}_2$ being the wave vectors of the Bragg photons). We measure the energy absorption spectrum $D(\omega)$ at a fixed momentum transfer $q \lesssim \pi/a$, where a is the periodicity of the lattice along the chains. We show how, with the precise knowledge of the particle dispersion in the high band [16,17], it is possible to obtain information about quasiparticle structure and dynamics in the MI. Moreover, a refined scheme would give access to a momentum-resolved absorption rate $D(k, \omega)$, which we show is directly related to the single-particle spectral function $A(k, \omega)$ in the lowest-energy band. From the latter, one obtains the Green's function (GF) of the MI, lending information on both spatial and temporal

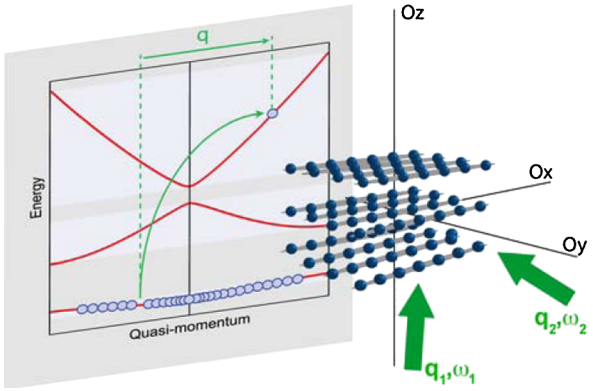

FIG. 1 (color online). An array of 1D gases created by a 2D optical lattice is driven into the MI state by a third (OL) in the Ox direction. The energy band structure in the 1D lattice is depicted on the left with red solid lines. The lowest band corresponds to particles in the MI, and above it are the higher single-particle energy bands. Two laser beams (Bragg beams, green arrows) excite the initial MI by transferring a particle to a high-energy band and leaving a hole in the many-body state.

coherence of quasiparticles. Such a measurement is analogous to angle-resolved photoemission spectroscopy used in solid-state [18], recently extended to ultracold gases through Raman [19,20] and rf spectroscopy [21].

We start by briefly describing the experimental setup used to obtain the interband spectra (details can be found in [7,22]). We load a Bose-Einstein condensate of ^{87}Rb in a 3D optical lattice at the wavelength $\lambda_L = 830$ nm. The amplitudes V_i of the lattices along each axis $i = x, y, z$ are expressed in units of the recoil energy $E_R = h^2/(2m\lambda_L^2)$, $V_i = s_i E_R$, where m denotes the mass of ^{87}Rb. The optical lattices are ramped up to their final values s_i with an exponential ramp of duration 140 ms and time constant 30 ms. Two lattice amplitudes ($s_y = s_z = 35$) are fixed to create an array of 1D chains. The amplitude of the third lattice s_x is varied to tune the ratio between the onsite interaction energy U and the tunneling amplitude J_1 between Wannier states of the lowest Bloch band in each 1D MI chain from $U/2J_1 \simeq 7$ to $U/2J_1 \simeq 42$.

The Bragg beams are derived from a laser at 780 nm, detuned by ~200 GHz from the D_2 line of ^{87}Rb. In this work we fix $q = 0.96(3)\pi/a$, and we measure the amount of excitations induced by the Bragg beams as a function of their frequency difference ω. The measured quantity $D(\omega)$ is the mean square width of the zero-momentum peak in a phase-coherent lattice gas obtained after lowering the 3D optical lattices. Timing and details of the experimental procedure can be found in [22], in particular the way $D(\omega)$ is rescaled with the parameters of the Bragg beams to allow a relative comparison of the different spectra. In [22], we also verified that $D(\omega)$ is proportional to the energy transferred to the gas so that it can be written as $D(\omega) = \mathcal{C}\omega S(q, \omega)$, where $\mathcal{C}$ is a constant independent of the lattice strength [23].

In Fig. 2(a), we show an example of the spectra obtained for lattice of amplitude $s_x = 9$ at frequencies resonant with transitions to the second and third Bloch bands. The total spectral weight $W = \int d\omega D(\omega)$ of transitions to the third band as a function of s_x is shown in Fig. 2(b). The suppression of spectral weight is due to reduction of the matrix element, or Frank-Condon overlap, between wave functions of the two bands with increasing lattice strength. The distribution of spectral weight within each band is primarily determined by two factors: (i) the density of final states (DOS) in that band and (ii) the particle-hole coherence in the Mott ground state driven by quantum fluctuations about the classical state with precisely n (integer) particles on each site. The peaks seen at the band edges, for example, are the result of the divergent DOS there. Furthermore, we quantify the asymmetry of the spectra about the band centers through the skewness (third moment) [24] of $S(q, \omega)$. This is shown in Figs. 2(c) and 2(d) for the second and third band as a function of s_x. A positive skewness corresponds to an imbalance toward lower energies. Using a theoretical model, we shall relate the skewness, and its

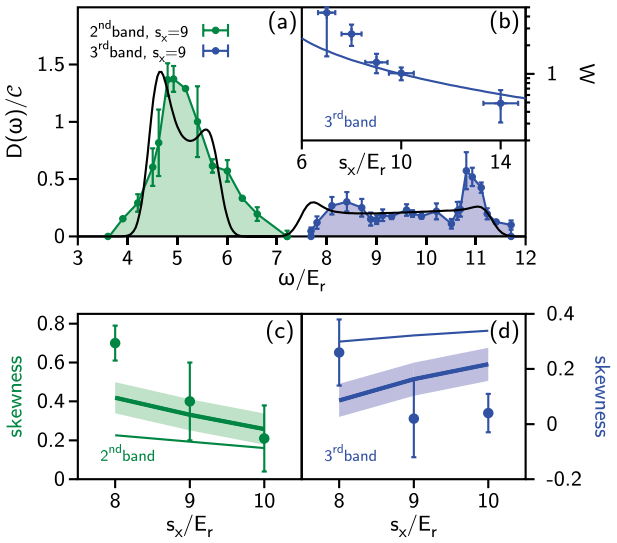

FIG. 2 (color online). Interband Bragg spectra. (a) Energy absorption rate $D(\omega)$ over the energy range of the second and third Bloch band for a Bragg momentum transfer $q = 0.96\pi/a$ and for a lattice depth $s_x = 9$. The (blue and green) dots are the experimental data with error bars indicating statistical uncertainties after averaging over four to five experimental acquisitions; the black lines are the theoretical predictions for $D(\omega)$. (b) Integrated spectral weight W in the third band. (c) and (d) Skewness (third moment) of $S(q, \omega)$ in the second (c) and third (d) band. The measured values are compared to the theoretical prediction including particle-hole coherence (thick lines) and to the contribution of the single-particle density of states alone (thin lines). The shaded area indicates the systematic uncertainty in determination of s_x in the experiment.

variation with band index and lattice amplitude, to the particle-hole coherence in the Mott state.

The Bragg perturbation couples to the particle density and, in the linear response regime, the excitation rate $D(\omega)$ is directly related to the dynamic structure factor

$$S(q, \omega) = \sum_m |\langle m|\rho_q|0\rangle|^2 \delta(\omega - \omega_{m0}) = \mathrm{Im}[\Pi(q, \omega)], \quad (1)$$

where ρ_q is the density operator at momentum q [25]. The sum runs over excited states, and $\hbar\omega_{m0}$ is the associated excitation energy.

The response function $\Pi(q, \omega)$ is represented graphically by the bubble diagram in Fig. 3(a): (i) the vertex describes the coupling of the Bragg beams to the density operator ρ_q; (ii) the full line is the GF of the hole produced in the lowest band by the Bragg excitation; (iii) the dashed line represents the GF of the particle excited to the nth band; (iv) the filled area is the T-matrix for scattering of the upper-band particle with the hole in the lowest band. We explain how we evaluate each part of the diagram, showing that for excitations to the higher bands the contribution of the final-state interaction can be neglected; hence, the process can be well described by the bare bubble shown in Fig. 3(c). Since without this interaction the propagation

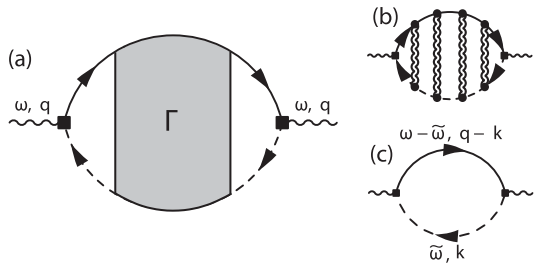

FIG. 3. Response functions. (a) Diagram describing the Bragg excitation in the linear response. The black squares describe the coupling of the Bragg beams to the density fluctuations. The full (dashed) lines denote the GF of a hole in the MI (of an upper band particle). The gray area Γ stands for the final-state interactions between the upper band particle and the MI hole. (b) In a T-matrix approximation, the final state interaction gives rise to a ladder diagram, where the wiggly lines denote the interaction between the upper band particle and the hole. (c) In the absence of final state interactions, the bare bubble describes the experimental response.

of the upper band particle can be calculated as the one of a free particle, the experiment effectively probes the remaining unknown which is related to the single-particle GF.

Let us first consider the edge vertices which correspond to the matrix element for the excitation of a particle from the lowest to the upper band by the density operator. To find this matrix element, we express the field operators in terms of creation operators in Wannier states of the lattice sites, so that $\rho(x) = \sum_{ij,nm} w^*_{mj}(x) w_{ni}(x) b^\dagger_{ni} b_{mj}$, where n, m are band indices, i, j site indices, and $w_{ni}(x)$ the respective Wannier functions. From now on, we assume that the lattice is sufficiently deep that the overlap between Wannier functions of neighboring sites can be neglected in the density operator. In addition, we focus on the component of the density operator that induces transitions from the lowest to the nth band:

$$\rho_n(q) = \bar{\rho} F_{1n}(q) \sum_i e^{-iqR_i} b^\dagger_{ni} b_{1i}, \tag{2}$$

where R_i is the position at site i, and $\bar{\rho}$ the filling of the MI. $F_{1n}(q)$ is the matrix element

$$F_{1n}(q) = \int dx w_{1i}(x) e^{-iqx} w_{ni}(x) \approx \frac{(-iql_0)^n}{\sqrt{2^n n!}} e^{-((ql_0)^2/4)}. \tag{3}$$

To get a simple expression for the dependence of $F_{1n}(q)$ on the lattice strength, we approximated the Wannier states by those of a harmonic well with oscillator length $l_0 = \lambda/(2\pi s_x^{1/4})$; however, for the comparison with experimental results, we use the exact Wannier functions [17].

To describe the hole propagation in the MI, we use the generalized Bogoliubov theory [14,26], which accounts for quadratic quantum fluctuations (i.e., virtual particles and holes) about the classical (Gutzwiller) ground state. The particle operator in the lowest band can be represented in terms of the Bogoliubov quasiparticle and quasihole excitations as $b_k = \sqrt{f(k)}(\beta^\dagger_{h,k} + \beta_{p,k})$, which are a combination of an added particle (doublon) and removed hole on the Mott background, e.g., $\beta^\dagger_{p,k} = u_k p^\dagger_k + v_k h_{-k}$ and $f(k) = (u_k - v_k)^2$. The ground state is the vacuum of the operators $\beta_{p/h,k}$. Therefore, $f(k) = \langle b^\dagger_k b_k \rangle$ is simply the momentum distribution. Accordingly, the single particle Green's function in the lowest Bloch band is given by:

$$G_1(k, i\omega) = \frac{f(k)}{i\omega - \omega_p(k)} + \frac{f(k)}{-i\omega - \omega_h(k)} \equiv G_p + G_h. \tag{4}$$

$\omega_p(k)$ [$\omega_h(k)$] denotes the dispersion relation of a particle [hole] in the lowest Bloch band. The momentum distribution $f(k)$ stems from quasiparticle coherence factors, and within the Bogoliubov theory it is

$$f(k) = \frac{1}{\sqrt{1 - \frac{J_1}{J_c}\cos k}}. \tag{5}$$

Here, J_c is the critical hopping strength at the Mott transition. We shall restrict ourselves to using the Bogoliubov theory deep in the Mott insulator, where it provides a good approximation of the single particle Green's function [27]. In this regime, $f(k) \approx 1 + \frac{1}{2}(J_1/J_c)\cos k$ to leading order in J_1/J_c.

The GF of a single particle in the nth upper band is taken to be that of a free particle with appropriate band dispersion $\tilde{\omega}_n(k)$. We take into account a slightly renormalized dispersion due to interaction with the background of filled sites of the MI [28].

The interaction between the particle in the upper band and the hole in the lowest band is included in the full T-matrix [filled box in Fig. 3(a)]. In general, this leads to a complicated sum of diagrams, including all possible sequences of multiple collisions through the interaction term $U_{1n} b^\dagger_{ni} b_{ni} (p^\dagger_i p_i - h^\dagger_i h_i)$. Here, we represented the interaction in terms of actual particles and holes in the classical ground state, where U_{1n} is the interaction matrix element between Wannier states of the lowest and the nth band. The interaction looks more complicated when expressed in terms of the Bogoliubov quasiparticles and quasiholes. However, the sum simplifies in the strong lattice limit when $v_k \ll u_k$. Then, to leading order in v_k, we can include only the ladder diagrams shown in Fig. 3(b), which are easily summed up as a geometric series [28]. The result of the interaction, treated by the ladder summation, is to induce a bound state between the upper band particle and the hole in the MI [28]. For the experimental parameters, the weight carried by this bound state ($< 1\%$) is too small to affect the measurements. We conclude that to an excellent approximation, we can use the bare bubble diagram shown in Fig. 3(c) to compute the structure factor.

The structure factor computed from the bare bubble diagram is given by

$$S(q,\omega) = \bar{\rho}^2 |F_{1n}|^2 \int \frac{dk}{2\pi} \quad A_h(k-q, \omega - \tilde{\omega}_n(k)), \quad (6)$$

where $A_h(k,\omega) = -\pi^{-1}\mathrm{Im}G_h(k, \omega + i0^+)$ is the hole spectral function in the Mott insulator. In particular, the spectral function obtained from the generalized Bogoliubov theory of the Mott insulator is $A_h(k,\omega) = f(k)\delta[\omega - \omega_h(k)]$.

This is the formula we use to compare with the experiment. However, to clearly reveal the two important factors in the spectra, it is worth making another simplification. In the regime of interest, of strong optical lattice, the bandwidth of the hole in the lowest band can be neglected compared to the dispersion of a particle in the excited band, and we can take $\omega_h(k) = \omega_0$. This leads to

$$S(q,\omega) \approx \bar{\rho}^2 |F_{1n}(q)|^2 \rho_n(\omega - \omega_0) f(k_n(\omega - \omega_0) - q), \quad (7)$$

$\rho_n(\omega)$ being the single particle DOS in the nth band and $k_n(\omega)$ the inverse function of the dispersion in that band $\omega_n(k)$.

In the limit of infinitely deep lattice $f(k) \to 1$, and the observed line shape is determined solely by the single particle DOS. With reduction of the lattice amplitude (increased hopping), $f(k)$ becomes more strongly peaked near $k = 0$ and, therefore, contributes more significantly to the line shape. Specifically, it gives increased weight to frequencies resonant with transitions that create a Mott hole near $k = 0$ and an excited nth band particle with quasimomentum q. If we take $q \approx \pi/a$, as in the experiment, this effect enhances the weight of transitions that create a higher band particle near the Brillouin zone edge. From the band structure shown in Fig. 1, it is clear that in this way the momentum distribution skews the spectra of the second band toward lower energies and those of the third band toward higher energies. It should be noted, however, that the single-particle DOS is itself not symmetric about the band centers. In particular, for both the second and third band, the peak of the DOS is skewed toward lower energies (positive skewness). Therefore, the effect of coherence in the Mott insulator is to increase the skewness of the second band and decrease it in the third band spectra.

Using Eq. (6), we calculate the experimental observable $D(\omega) = \mathcal{C}\omega S(q,\omega)$. The proportionality constant $\mathcal{C}$ is fixed by matching the integrated spectral weight of excitations to the third band W for a single value of the lattice strength ($s_x = 10$). We use the same constant to compute the spectra for all other lattice amplitudes and for all the bands. In addition, we broaden the delta function in Eq. (6) to effectively account for the trap-confining potential [29].

The spectrum obtained in this way is presented and compared to the experimental results in Fig. 2(a) for $s_x = 9$. Note that there are no free parameters except the overall proportionality constant C which was calibrated once. We attribute the relative shift of the spectra to the systematic uncertainty in the actual lattice amplitude in the experiment [30]. The calculated total weight of absorption W, shown in Fig. 2(b), is in good agreement with the experimental data. The reduction of W with increasing lattice strength is due to suppression of the Frank-Condon factor F_{1n}.

As discussed above, the skewness of the structure factor relative to that of the pure single particle density of states is a direct measure of the quasiparticle coherence factor in the Mott insulator. Figures 2(c) and 2(d) compare the measured skewness [24] of $S(q,\omega)$ in the second and third bands to that calculated from the theoretical spectra (thick lines). Both are compared to the skewness of the single particle DOS in the corresponding bands. As anticipated, the actual skewness is consistently higher than the pure DOS effect in the second band and lower than the DOS effect in the third band, and this effect is observed in a systematic way for different lattice amplitudes. This disagreement of the experimental data with the single-particle theory [31] is a clear indication of coherence effects inside the MI.

To conclude, we have shown that the interband Bragg absorption spectrum, in the linear response regime, gives information on the single-particle Green's function. In particular, we have quantified the single-hole coherence through analysis of the asymmetry of the spectra.

It is important to note that the structure factor is related, through Eq. (6), to a rather complicated weighted sum over the hole spectral function and is not proportional to the spectral function itself. For this reason, input from a theoretical model of the Green's function in the Mott insulator was needed to extract a measure of the hole coherence. For this we used a Bogoliubov-like theory that takes into account zero-point fluctuations around the mean-field Mott wave function. The nontrivial hole coherence stems from these zero-point fluctuations.

It would be interesting to directly measure the single-hole spectral function and, thereby, obtain quasiparticle energies, coherence factors, and decay times in a model independent way. We suggest that, in principle, this can be done using a band-mapping technique [32]. By counting how many particles are excited to a particular k state in the upper band, we would eliminate the k integral in Eq. (6). Then, the response function corresponding to the excitation rate per final momentum k would be

$$S_{1n}(q,k,\omega) = \bar{\rho}^2 |F_{1n}(q)|^2 A_h(k-q, \omega - \tilde{\omega}_n(k)). \quad (8)$$

This theoretical description of the measurement process is identical to the description of angle-resolved photoemission spectroscopy [33,34], a method that is currently used extensively to measure the electronic spectral function of interesting materials [18]. Our proposed scheme could also be implemented on more complex many-body ground-states in a lattice.

This work was supported by ISF, MAE-MIUR (Joint Laboratory LENS-Weizmann), ECR Firenze, by ERC through the DISQUA grant, and by MIUR through PRIN2009. S. D. H acknowledges support by the Swiss Society of Friends of the Weizmann Institute of Science.

*fabbri@lens.unifi.it
†sebastian.huber@weizmann.ac.il
‡Present address: Laboratoire Charles Fabry, 2 avenue Agustin Fresnel, 91127 Palaiseau Cedex, France.

[1] M. Greiner, O. Mandel, T. Esslinger, T. W. Hänsch, and I. Bloch, Nature (London) **415**, 39 (2002).
[2] T. Stöferle, H. Moritz, C. Schori, M. Kohl, and T. Esslinger, Phys. Rev. Lett. **92**, 130403 (2004).
[3] S. Fölling, F. Gerbier, A. Widera, O. Mandel, T. Gericke, and I. Bloch, Nature (London) **434**, 481 (2005).
[4] G. K. Campbell, J. Mun, M. Boyd, E. W. Streed, W. Ketterle, and D. E. Pritchard, Phys. Rev. Lett. **96**, 020406 (2006).
[5] I. B. Spielman, W. D. Phillips, and J. V. Porto, Phys. Rev. Lett. **100**, 120402 (2008).
[6] X. Du, S. Wan, E. Yesilada, C. Ryu, D. J. Heinzen, Z. Liang, and B. Wu, New J. Phys. **12**, 083025 (2010).
[7] D. Clément, N. Fabbri, L. Fallani, C. Fort, and M. Inguscio, Phys. Rev. Lett. **102**, 155301 (2009).
[8] W. S. Bakr, A. Peng, M. E. Tai, R. Ma, J. Simon, J. I. Gillen, S. Fölling, L. Pollet, and M. Greiner, Science **329**, 547 (2010).
[9] J. F. Sherson, C. Weitenberg, M. Endres, M. Cheneau, I. Bloch, and S. Kuhr, Nature (London) **467**, 68 (2010).
[10] U. Bissbort, S. Götze, Y. Li, J. Heinze, J. S. Krauser, M. Weinberg, C. Becker, K. Sengstock, and W. Hofstetter, Phys. Rev. Lett. **106**, 205303 (2011).
[11] S. Sachdev, *Quantum Phase Transitions* (Cambridge University Press, Cambridge, England, 1999).
[12] A. Iucci, M. A. Cazalilla, A. F. Ho, and T. Giamarchi, Phys. Rev. A **73**, 041608(R) (2006).
[13] A. M. Rey, P. B. Blakie, G. Pupillo, C. J. Williams, and C. W. Clark, Phys. Rev. A **72**, 023407 (2005).
[14] S. D. Huber, E. Altman, H. P. Büchler, and G. Blatter, Phys. Rev. B **75**, 085106 (2007).
[15] J. Heinze, S. Götze, J. S. Krauser, B. Hundt, N. Fläschner, D.-S. Lühmann, C. Becker, and K. Sengstock, Phys. Rev. Lett. **107**, 135303 (2011).
[16] M. Abramowitz and I. Stegun, *Handbook of Mathematical Functions* (Dover, New York, 1965), p. 720, Sect. 20.
[17] W. Zwerger, J. Opt. B **5**, S9 (2003).
[18] A. Damascelli, Z. Hussain, and Z.-X. Shen, Rev. Mod. Phys. **75**, 473 (2003).
[19] T.-L. Dao, A. Georges, J. Dalibard, C. Salomon, and I. Carusotto, Phys. Rev. Lett. **98**, 240402 (2007).
[20] T.-L. Dao, I. Carusotto, and A. Georges, Phys. Rev. A **80**, 023627 (2009).
[21] J. T. Stewart, J. P. Gaebler, and D. S. Jin, Nature (London) **454**, 744 (2008).
[22] D. Clément, N. Fabbri, L. Fallani, C. Fort, and M. Inguscio, New J. Phys. **11**, 103030 (2009).
[23] A. Brunello, F. Dalfovo, L. Pitaevskii, S. Stringari, and F. Zambelli, Phys. Rev. A **64**, 063614 (2001).
[24] The skewness is defined as $\gamma = \frac{1}{W\sigma^3}\int d\omega(\omega - \bar{\omega})^3 S(q,\omega)$, where $\sigma^2 = \frac{1}{W}\int d\omega(\omega - \bar{\omega})^2 S(q,\omega)$ and $\bar{\omega} = \frac{1}{W}\int d\omega\omega S(q,\omega)$.
[25] J. Stenger, S. Inouye, A. P. Chikkatur, D. M. Stamper-Kurn, D. E. Pritchard, W. Ketterle, Phys. Rev. Lett. **82**, 4569 (1999).
[26] E. Altman and A. Auerbach, Phys. Rev. Lett. **89**, 250404 (2002).
[27] On approaching the transition, the Bogoliubov expression of the single-particle Green's function suffers from being a nonconserving approximation. The expression for density response function does not suffer from the same problem [14].
[28] See Supplemental Material at http://link.aps.org/supplemental/10.1103/PhysRevLett.109.055301 for more information regarding strong-coupling mean-field description of Mott insulators and final-state interactions.
[29] A broadening on the order of the chemical potential ($\sim$ 800 Hz) is needed because the Bragg beams have non-vanishing matrix elements between states in different locations of the trap.
[30] Note that a relative frequency shift between the experimental data points and the theoretical curves can be explained as a result of the 10% systematic uncertainty in the lattice height calibration. As a matter of fact, the position of the third Bloch band shifts by 0.3Er (0.4Er), passing from $s = 8$ to $s = 8.8$ ($s = 10$ to $s = 11$).
[31] At a level of confidence greater than 99.5%.
[32] M. Greiner, I. Bloch, O. Mandel, T. W. Hansch, and T. Esslinger, Phys. Rev. Lett. **87**, 160405 (2001).
[33] C. Caroli, D. Lederer-Rozenblatt, B. Roulet, and D. Saint-James, Phys. Rev. B **8**, 4552 (1973).
[34] G. D. Mahan, *Many-Particle Physics* (Plenum Press, New York, 1990).